ESC European Society of Cardiology

European Heart Journal - Cardiovascular Imaging (2019) **20**, 668–676
doi:10.1093/ehjci/jey175

Metabolic pathways associated with right ventricular adaptation to pulmonary hypertension: 3D analysis of cardiac magnetic resonance imaging

Mark I. Attard[1,2], Timothy J.W. Dawes[1,2,3], Antonio de Marvao[1], Carlo Biffi[1,4], Wenzhe Shi[1,4], John Wharton[2], Christopher J. Rhodes[2], Pavandeep Ghataorhe[2], J. Simon R. Gibbs[3], Luke S.G.E. Howard[5], Daniel Rueckert[4], Martin R. Wilkins[2], and Declan P. O'Regan[1]*

[1]MRC London Institute of Medical Sciences, Du Cane Road, London W12 0NN, UK; [2]Division of Experimental Medicine, Department of Medicine, Imperial College London, Du Cane Road, London W12 0NN, UK; [3]Royal Brompton Cardiovascular Research Centre, National Heart & Lung Institute, Imperial College London, Dovehouse Street, London SW3 6LY, UK; [4]Department of Computing, Imperial College London, South Kensington Campus, Queen's Gate, London SW7 2RH, UK; and [5]Imperial College Healthcare NHS Trust, Du Cane Road, London W12 0NN, UK

Received 24 August 2018; editorial decision 23 October 2018; accepted 27 October 2018; online publish-ahead-of-print 7 December 2018

Aims We sought to identify metabolic pathways associated with right ventricular (RV) adaptation to pulmonary hypertension (PH). We evaluated candidate metabolites, previously associated with survival in pulmonary arterial hypertension, and used automated image segmentation and parametric mapping to model their relationship to adverse patterns of remodelling and wall stress.

Methods and results In 312 PH subjects (47.1% female, mean age 60.8 ± 15.9 years), of which 182 (50.5% female, mean age 58.6 ± 16.8 years) had metabolomics, we modelled the relationship between the RV phenotype, haemodynamic state, and metabolite levels. Atlas-based segmentation and co-registration of cardiac magnetic resonance imaging was used to create a quantitative 3D model of RV geometry and function—including maps of regional wall stress. Increasing mean pulmonary artery pressure was associated with hypertrophy of the basal free wall ($\beta = 0.29$) and reduced relative wall thickness (β = -0.38), indicative of eccentric remodelling. Wall stress was an independent predictor of all-cause mortality (hazard ratio = 1.27, $P = 0.04$). Six metabolites were significantly associated with elevated wall stress ($\beta = 0.28$–0.34) including increased levels of tRNA-specific modified nucleosides and fatty acid acylcarnitines, and decreased levels (β = -0.40) of sulfated androgen.

Conclusion Using computational image phenotyping, we identify metabolic profiles, reporting on energy metabolism and cellular stress-response, which are associated with adaptive RV mechanisms to PH.

Keywords pulmonary hypertension • metabolomics • wall stress • cardiac magnetic resonance imaging • image segmentation • machine learning

Introduction

Right ventricular (RV) failure complicates a diverse group of cardiorespiratory diseases. It is the strongest determinant of survival in pulmonary arterial hypertension (PAH), and independently predicts outcome in pulmonary hypertension (PH) secondary to left heart failure, chronic lung disease, or thrombo-embolic disease.[1] Initially, there is a compensatory phase where the RV maintains efficient energy

* Corresponding author. Tel: +44 020 33133298; Fax: +44 020 33133038. E-mail: declan.oregan@imperial.ac.uk

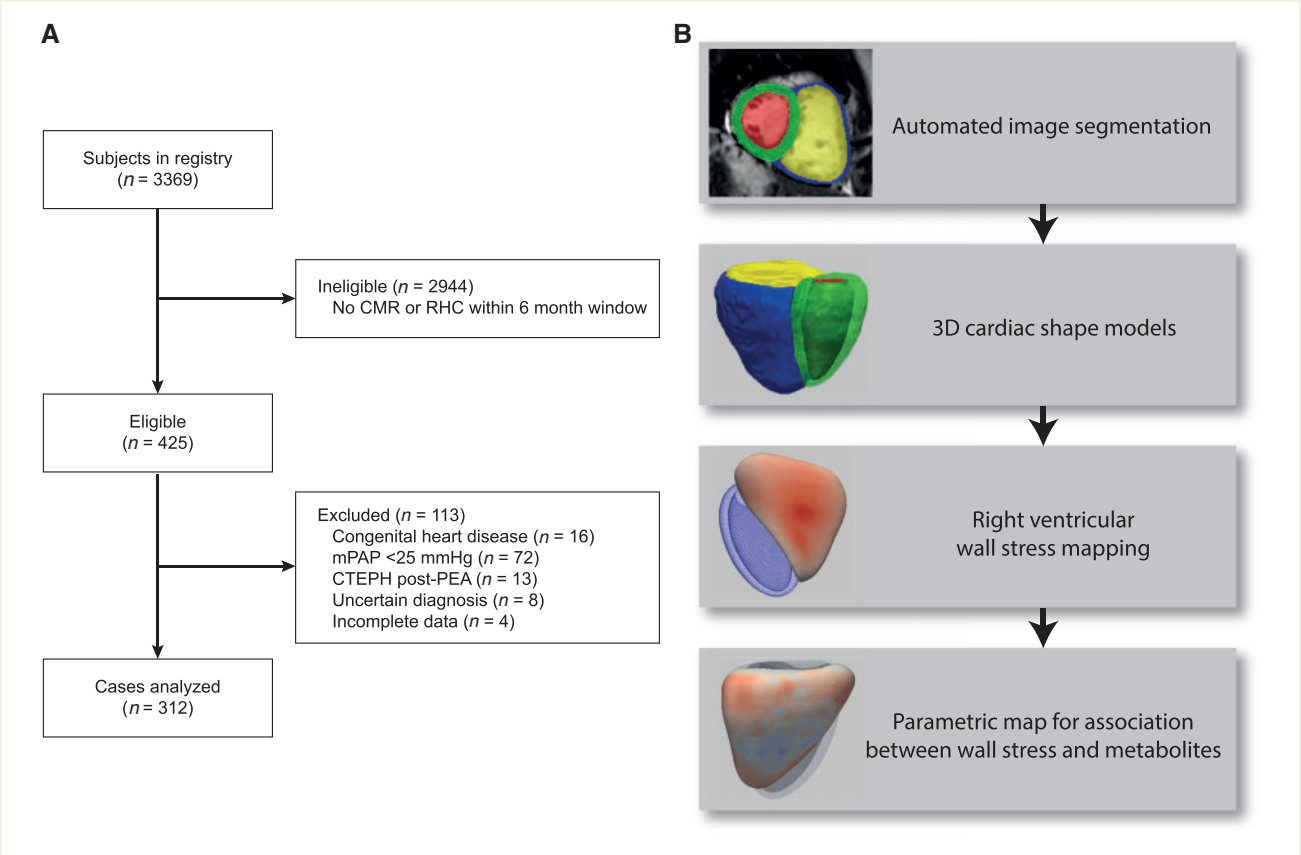

Figure 1 Study design. (*A*) Flowchart to show the patients included in the study. (*B*) Flowchart of the image analysis steps from automated CMR segmentation, shape modelling, and statistical parametric mapping. CMR, cardiac magnetic resonance imaging; CTEPH, chronic thromboembolic pulmonary hypertension; mPAP, mean pulmonary artery pressure; RHC, right heart catheterization; PEA, pulmonary endarterectomy.

transfer by an adaptive increase in wall thickness (WT) and contractility,[2] until the more advanced stages of disease when the RV dilates, wall stress rises, and ventriculo-arterial uncoupling occurs leading to heart failure.[3] However, RV failure associated with PH is not simply a predictable consequence of increased afterload. Patients may show a progressive decline in RV function despite a therapeutic response in pulmonary vascular resistance,[4] and data from animal models suggest a role for circulating mediators that interfere with adaptive RV mechanisms to elevated mechanical stress.[5]

It has recently been recognized that translational regulation and energy metabolism are disturbed in PAH and that monitoring of plasma metabolites that report on these pathways could be useful to assess disease progression and response to therapy.[6] While metabolomics provides novel molecular insights into the pathogenesis of disease it is unknown if metabolic phenotyping, as well as predicting survival, could identify key pathways for mechanisms that influence myocardial adaptation to afterload. To examine this, we developed an automated method for 3D biomechanical modelling of the right ventricle using clinical cardiac magnetic resonance imaging (CMR)—and combined this with robust statistical techniques for mapping the strength of association between circulating biomarkers and regional wall stress. Our aim was to determine if molecular profiles, known to be predictive of survival, are associated with evidence of adverse RV remodelling and biomechanical stress in patients with PH.

Methods

Study population

The study was approved by the Heath Research Authority and all participants gave written informed consent. Patients referred between 2002 and 2015 to Imperial College Healthcare NHS Trust (London, UK), Hammersmith Hospital for routine diagnostic assessment of PH including cardiac imaging were included. A diagnosis of PH was made according to standard guidelines with a resting mean pulmonary artery pressure (mPAP) ≥25 mmHg by right heart catheterization (RHC),[7] performed using standard Swan Ganz catheters introduced via an internal jugular, subclavian, or femoral vein approach. Exclusion criteria were PH due to congenital heart disease, previous pulmonary endarterectomy, or more than 6 months between baseline investigations. Disease classification was according to the Dana Point system.[8] All patients were treated with standard therapy in accordance with current guidelines.[7] A reference set of imaging in a large cohort of healthy control subjects was taken from the UK Digital Heart Project (https://digital-heart.org/).[9]

Study design

A flowchart of the patients recruited to the study and the steps in image processing are shown in *Figure 1*. We used automated computational image analysis to create a biomechanical model of the heart from CMR images in patients with PH. We then modelled the relationship between

haemodynamic parameters and 10 candidate metabolites, previously shown to be associated with outcome in PAH,[6] on the structure and function of the right ventricle across all PH groups. Lastly, we assessed the relationship between RV wall stress and survival.

Imaging

CMR imaging to assess biventricular function was performed according to a standard clinical protocol.[10] Imaging was performed on a 1.5T Philips Achieva (Best, Netherlands) and stored on an open-source database.[11] Conventional manual volumetric analysis was performed using commercial cardiac analysis software to a standard published protocol.[12] Indexed RV end-diastolic and end-systolic volumes were calculated and indexed stroke volume and ejection fraction (RVEF) derived. Papillary muscles and trabeculae were included in the cavity volume. Indexed RV mass (RVMI) excluded the interventricular septum. Ventricular mass index (VMI), or Fulton's index, was the ratio of RV mass to left ventricular mass index (including the interventricular septum).[13] All mass and volume measurements were indexed to body surface area (BSA) estimated by the Mosteller formula.

Three-dimensional image analysis

All image processing was performed in Matlab (Mathworks, Natick, MA, USA). We took the short-axis cines for each PH patient and automatically aligned them by minimizing the intensity differences between each slice. Prior knowledge for the supervised machine learning segmentation algorithm comprised manually-annotated images at end diastole and end-systole in 57 PH patients, complementing the UK Digital Heart Project atlases, to extend accurate analysis of both shape and motion to RV-overload phenotypes.[9] Each voxel in the PH atlases was assigned five labels (LV/RV cavity or myocardium, and background) using freely available software (ITKsnap, National Library of Medicine's Insight Segmentation and Registration Toolkit). A multi-atlas approach utilized the entire dataset of labelled atlases rather than relying on a model-based average representation.[14] An approximate graph search was performed to find correspondences between small cubic regions, or patches, in the image to be segmented and the database of labelled atlases. Spectral embedding, using a multi-layered graph of the images, captured global shape properties of the heart. Finally, we estimated anatomical patch correspondences based on a joint spectral representation of the image and atlases.[15,16] The final segmentations were co-registered to an average template surface mesh, where vertex density was determined by the curvature at each sampling point, allowing cardiac shape or function within the population to be compared in a common space.

This resulted in a statistical model describing within-population spatial variation in RV geometry at approximately 20 000 vertices. The right ventricular inlet, outlet and apical/trabecular regions were also demarcated on the template image. WT was calculated as the distance between the endocardial and epicardial surfaces perpendicular to a mid-wall plane. Relative wall thickness refers to WT corrected for variation in ventricular volume following a scale transformation of the right ventricle. Curvature tensors were derived using an algorithm that estimates the curvature of a smooth surface from a sampled polyhedral approximation.[17] Excursion was defined as the distance between corresponding anatomical points at end-systole and end-diastole.[18] Geometric variation in RV shape was quantified by vertex-wise comparison to a mean template derived from our reference population of healthy adults.

The segmentation algorithms and template mesh are freely available at https://github.com/UK-Digital-Heart-Project/PHsegment.

Metabolomics

Venous blood samples were put on ice, centrifuged (1300*g*, 15 min) within 30 min and stored at -80°C. Metabolomic profiling by ultra-performance liquid chromatography mass spectrometry was conducted by Metabolon (Durham, NC, USA), which provided semi-quantitative assessment of 949 named and 467 unnamed metabolite levels, annotated with pathways.

For the present study, we considered 10 candidate metabolites that had previously been identified as both discriminating PAH patients from symptomatic controls independent of confounding factors and being predictive of survival.[6] These metabolites were dehydroepiandrosterone sulfate (DHEA-S), N2,N2-dimethylguanosine (N2DMG), N1-methylinosine (N1MI), 3-hydroxy-3-methylglutarate (3H3MG), N-acetylmethionine (NAM), N-formylmethionine (NFM), fumarate (FMR), 1-linoleoyl-2-eicosapentaenoyl-GPC (18:2/20:5) (1L2EP), sphingomyelin (d18:1/20:0, d16:1/22: 0) (SM), and N-acetyltaurine (NAT). Data for creatinine and bilirubin were also recorded as these were found to be the most common confounders associated with metabolite levels.[6]

Right ventricular wall stress

Wall stress is a measure of the effect of hydraulic load on the myocardium and depends on the interaction between central pressure and the instantaneous geometry of the heart. We used an approach for modelling wall stress based on earlier work on the left ventricle in dilated cardiomyopathy.[19] We used a modified Laplace formula that, in contrast with the Young–Laplace law, does not assume that WT is negligible.[20] Wall stress was derived from the invasive systolic pulmonary artery pressure (sPAP), regional inner radius of curvature (*R*), and the corresponding end-systolic WT at each vertex using the following equation:

$$\text{Wall stress} = 0.133 \times \text{sPAP} \times \frac{R}{2WT \times \left(1 + \frac{WT}{2R}\right)}$$

A conversion factor of 0.133 was used to express the results in kN/m^2. Wall stress values were calculated for each vertex in the 3D model.

Statistical analysis

Data were analysed in R version 3.4.0 using RStudio Server version 1.043 (Boston, MA, USA). Variables were expressed as percentages if categorical, mean ± standard deviation if continuous and normal, and median ± interquartile range (IQR) if continuous and non-normal. We used statistical parametric mapping to visualize the strength of association between metabolomics markers and patterns of regional wall stress. We did this by fitting univariate regression models at each vertex of the 3D cardiac mesh—a method which has been previously validated using both clinical and synthetic data.[21] We adjusted for the following covariates: age, sex, ethnicity, BSA, PH group, and time from diagnosis. The metabolite relationships were further corrected for creatinine and bilirubin. We used a robust approach to inference, in which a consensus is drawn from multiple random data parcellations prior to permutation testing (Supplementary data online, *Figure S1*).[22] Multiple testing correction was achieved by controlling the false discovery rate to 5% using the Benjamini–Hochberg[23] procedure with models corrected jointly.[24] RV regions where the association between variables was significant ($P < 0.05$) were reported by the maximum β coefficient and the percentage area of RV free wall within the significance threshold.

The performance of RV wall stress as a predictor of survival was tested using a Cox proportional hazards multiple regression analysis (using the first principal component of the 3D wall stress data) with all-cause

Table 1 Summary of baseline patient characteristics

	All PH patients	PH patients with metabolomics	Healthy controls
N	312	182	1985
Age	60.8 ± 15.9	58.6 ± 16.8	42.2 ± 13.2
Female sex (%)	47.1	51.1	55.2
Body surface area (m^2)	1.86 ± 0.25	1.9 ± 0.3	1.82 ± 0.21
Ethnicity, *n* (%)			
Caucasian	248 (79.5)	152 (83.5)	1379 (69.5)
South Asian	14 (4.5)	8 (4.4)	305 (15.4)
African Black	20 (6.4)	7 (3.8)	211 (10.6)
Others	30 (9.6)	15 (8.2)	90 (4.5)
PH group[a], *n* (%)			
Pulmonary arterial hypertension	99 (31.7)	72 (39.6)	
PH due to left heart disease	42 (13.5)	7 (3.8)	
PH due to lung disease	12 (3.8)		
CTEPH	150 (48.1)	103 (56.6)	
PH with unclear mechanisms	9 (2.9)		
Functional			
Six-minute walk distance (m)	259.6 ± 157.8	276 ± 156.4	
WHO/NYHA functional class, I/II/III/IV	3/39/220/50	1/28/124/29	
Baseline haemodynamics			
Pulmonary capillary wedge pressure (mmHg)	13.8 ± 6.1	10.9 ± 7.2	
Mean pulmonary artery pressure (mmHg)	44.5 ± 13.2	46.7 ± 13.3	
Pulmonary vascular resistance (Woods units)	8.5 ± 5.5	9.3 ± 5.9	
Cardiac index (L/min/m^2)	2.4 ± 0.9	2.3 ± 0.9	
Volumetry			
RV end-diastolic volume (mL)	194.1 ± 72.4	196.1 ± 69.1	164.0 ± 38.3
RV end-diastolic volume (indexed) (mL/m^2)	105.2 ± 40	106.2 ± 39.4	89.3 ± 15.8
RV stroke volume (mL)	73.8 ± 28.3	69.8 ± 27.2	94.5 ± 20.2
RV stroke volume (indexed), (mL/m^2)	40.1 ± 15.9	37.7 ± 15.4	51.6 ± 8.3
RV ejection fraction (%)	40.5 ± 13.6	37.8 ± 13.4	58.2 ± 5.9
RV mass (g)	49.2 ± 15.3		

Variables are shown for the entire UK group and those with metabolomics as well as the healthy controls.
Values are expressed as mean ± standard deviation.
CTEPH, chronic thromboembolic PH; NYHA, New York Heart Association; PH, pulmonary hypertension; RV, right ventricle.
[a]Dana Point classification.

mortality as the outcome variable. Survival was defined as the time between date of the CMR imaging and death from any cause.

Results

We report data from 312 PH subjects (47.1% female, mean age 60.8 ± 15.9 years), of which 182 (51.1% female, mean age 58.6 ± 16.8 years) had metabolomics (within a median 11 months of CMR), in whom we modelled the relationship between RV phenotype, haemodynamic state, and the pre-defined metabolites. Imaging in 1985 healthy volunteers (55.2% female, mean age 42.2 ± 13.2 years) was used as a normal reference for ventricular geometry. In all subject groups, segmentation was successful and no data were excluded from analysis. Baseline characteristics are given in *Table 1*.

Three-dimensional phenotypes

The 3D phenotypic characteristics of the right ventricle are shown in *Figure 2* and summary variables by anatomic region in Supplementary data online, *Table S1*. Median RV WT was 3.0 mm (IQR 2.6–3.4 mm). The RV free wall in the inlet region had the greatest absolute (3.2, IQR 2.9–3.6 mm) and relative WT (3.1, IQR 2.7–3.4 mm). Compared with healthy adults the RV outflow showed the greatest regional expansion in shape (1.6, IQR -0.8 to 4.0 mm) with increased excursion (13.9, IQR 10.6–17.5 mm) and higher wall stress (43.5, IQR 28.0–66.7 kN/m^2). These comparisons, between apical/trabecular, inlet and outlet, were all significant ($P < 2.2 \times 10^{-16}$). Overall, median RV wall stress was 39.0 kN/m^2 (IQR 24.1–62.3 kN/m^2).

Maps showing the relationship between phenotypic variation and mPAP are shown in *Figure 3*. RVMI was positively associated with mPAP ($\beta = 0.13$, $P = 0.03$), and the strongest relationship between mPAP and WT was at the RV inlet ($\beta = 0.29$, significant area = 28% of

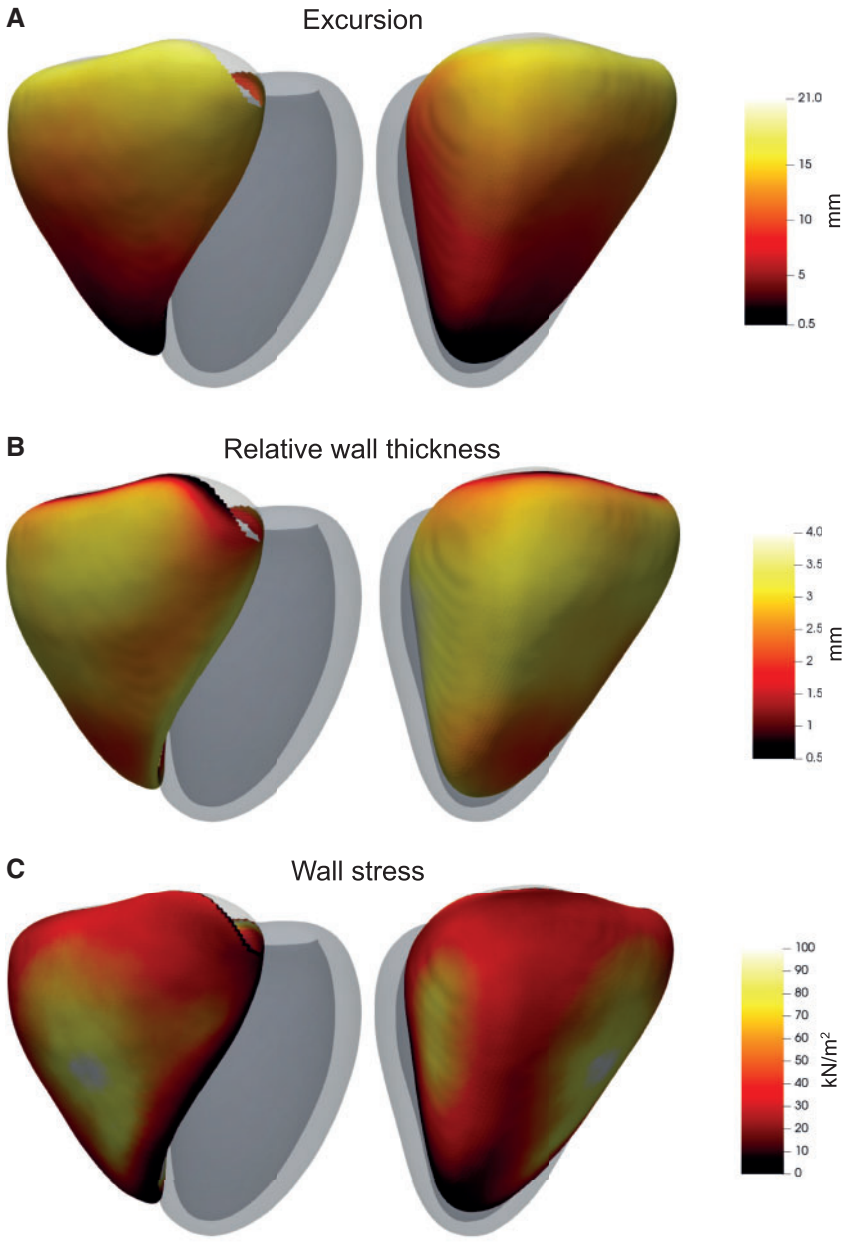

Figure 2 Three-dimensional models of the right ventricle in PH patients. Co-registered phenotypic data were used to create a map of RV features across the population. The RV is shown from two viewpoints with the left ventricle represented in grey. The median (*A*) systolic excursion, (*B*) relative wall thickness, and (*C*) wall stress at each corresponding anatomical point throughout the population ($n = 312$) is shown. These phenotypic data were then used in 3D regression models with haemodynamic variables or metabolomics levels as explanatory variables.

RV free wall). RVMI/RVEDVI was negatively associated with mPAP (β = -0.18, $P = 0.0007$) with a corresponding negative association between mPAP and relative WT throughout the free wall (β = -0.38, area = 88%). VMI, an indicator of remodelling,[25] was positively associated with mPAP ($\beta = 0.41$, $P = 8.9 \times 10^{-15}$). Patients' mPAP was positively associated with right ventricular end-diastolic volume (RVEDV) ($\beta = 0.23$, $P = 8.5 \times 10^{-5}$), corresponding to a global expansion in RV shape ($\beta = 0.29$, area = 95%). Regional systolic excursion was negatively associated with mPAP (β = -0.33, area = 73%). Wall stress and RVEF were inversely associated (β = -0.63, area = 97%) (Supplementary data online, *Figure S2*). RVEF itself was negatively associated with mPAP (β = -0.5, $P < 2 \times 10^{-16}$).

Metabolites associated with global variables and wall stress

The relationship between metabolite concentration and cardiac variables is shown in *Table 2*. Maps of the relationship between wall

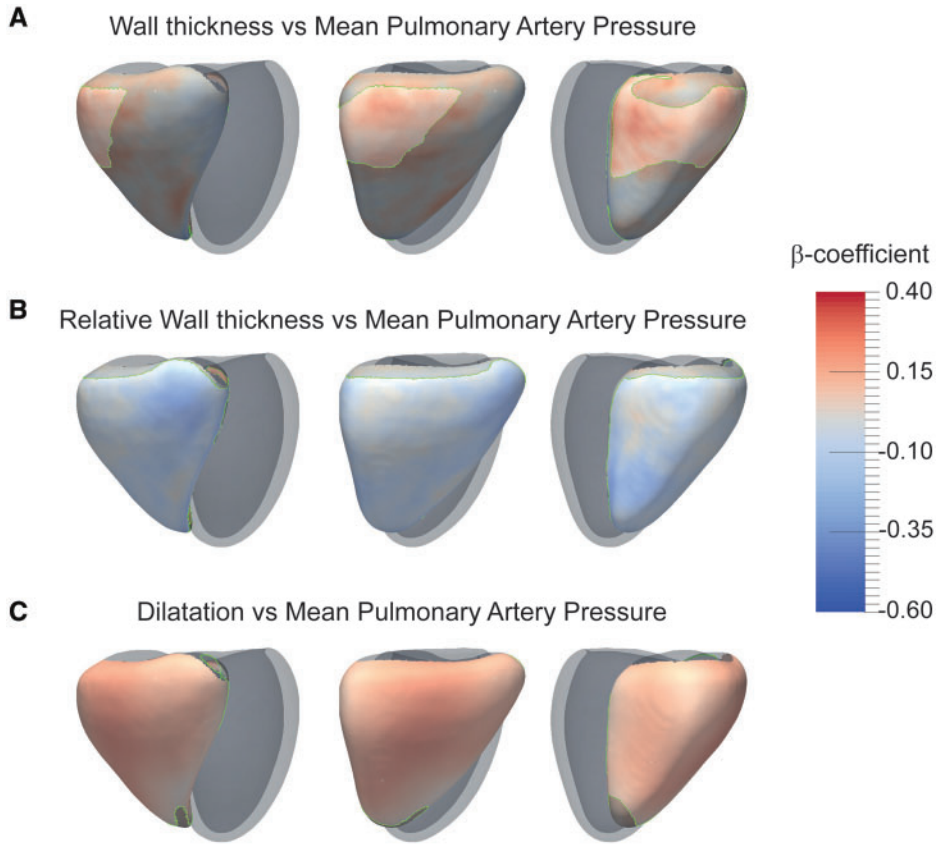

Figure 3 Statistical models of the right ventricle in PH patients. The strength of relationship between the stated variables is shown by 3D maps of standardized β coefficients with a significance threshold outlined in green. The RV is shown from three viewpoints with the left ventricle represented in grey. Relationships between mPAP and (*A*) wall thickness, (*B*) relative wall thickness, and (*C*) volume ($n = 312$). A positive regional relationship with mPAP is indicated in red and a negative relationship in blue. mPAP, mean pulmonary artery pressure.

stress and metabolites are shown in *Figure 4*, and Supplementary data online, *Figures S3* and *S4*. Of the 10 metabolites evaluated all except 1L2EP were significantly related to RVEF ($P < 0.05$), each with a negative association (β = -0.21 to -0.28) apart from DHEA-S which had a positive relationship ($\beta = 0.31$). Five of these metabolites were also positively associated with wall stress ($\beta = 0.28$–0.34), again with DHEA-S showing a negative association (β = -0.40), with at least 70% of the RV free wall reaching significance ($P < 0.05$). Metabolites were associated with a reduced RVM: RVEDV ratio indicating eccentric remodelling.

Survival

In multiple regression analysis, RV wall stress predicted survival independently of age, sex, BSA, time from diagnosis, and PH group (hazard ratio = 1.27, 95% confidence intervals 1.01–1.61, $P = 0.04$).

Discussion

We developed a fully automated approach for 3D modelling of the right ventricle in patients with PH enabling a comprehensive quantitative analysis of the complex relationship between elevated afterload, serum biomarkers and structural adaptation. We found that biomechanical overload, indicated by rising RV wall stress, is associated with altered levels of circulating biomarkers that report on energy metabolism and stress-response pathways. These results identify putative pathways that may influence RV adaptive mechanisms to elevated mechanical stress.

Integrative mathematical and statistical models of cardiac anatomy and physiology can play a vital role in understanding cardiac disease phenotypes and planning therapeutic strategies,[26] but previous work in this field has largely been confined to modelling the left ventricle. Here, we develop a powerful automated approach for modelling the geometry and function of the right ventricle in PH patients—enabling inferences about the relationship between biomarkers and complex cardiovascular phenotypes to be made within large populations. Invasive measurements in PH indicate that wall stress is the primary determinant of tissue oxygen consumption under adverse biomechanical conditions and the main driver of neurohumoral activation in myocytes.[27,28] We report the first results of 3D population mapping of wall stress in PH demonstrating strong regional variations across the freewall acting as a stimulus for adaptive myocardial hypertrophy and eccentric remodelling. We also observed that RVEF and wall stress were closely and inversely related to each other—reflecting

Table 2 Metabolite associations

Metabolite	Pathway	RVM	RVEDV	RVM/RVEDV	RVEF	VMI	3D wall stress
DHEA-S	Steroid	–	-0.26**	0.18*	0.31***	-0.21**	-0.4, 86.8%*
N2DMG	Purine, Guanine	–	0.18*	-0.17*	-0.28***	–	0.34, 73.1%*
N1MI	Purine, Hypo-Xanthine/Inosine	–	–	–	-0.21**	–	0.28, 87.2%*
3H3MG	Mevalonate	–	–	–	-0.25**	0.18*	0.32, 81.7%*
NAM	Met, Cys, SAM & Tau	–	–	-0.18*	-0.22**	–	0.31, 81.9%*
NFM	Met, Cys, SAM & Tau	–	0.17*	-0.14*	-0.23**	-0.17*	0.32, 69.7%*
Fumarate	TCA cycle	–	0.26**	-0.24**	-0.26**	0.22*	–
1L2EP	Phospholipid	–	–	–	–	–	–
SM	Sphingolipid	–	–	–	0.2*	-0.24**	–
NAT	Met, Cys, SAM & Tau	–	0.23*	-0.17*	-0.18*	–	–

Adjusted *P*-value:
*<0.05;**<0.01;***<0.001.
The relationship between metabolite concentration and phenotypic variables corrected for false discovery rate (presented as β coefficient with adjusted *P*-value, including area% for wall stress mapping).
3D, three-dimensional; DHEA-S, dehydroepiandrosterone sulfate; 3H3MG, 3-hydroxy-3-methylglutarate; 1L2EP, 1-linoleoyl-2-eicosapentaenoyl-GPC (18:2/20:5); NAM, N-acetylmethionine; NAT, N-acetyltaurine; NFM, N-formylmethionine; N1MI, N1-methylinosine; N2DMG, N2, N2-dimethylguanosine; RVEDV, right ventricular end-diastolic volume; RVEF, right ventricular ejection fraction; RVM, right ventricular mass; RVM/RVEDV, RVM corrected for RVEDV; VMI, ventricular mass index; SM, sphingomyelin (d18:1/20:0, d16:1/22:0); –, not significant.

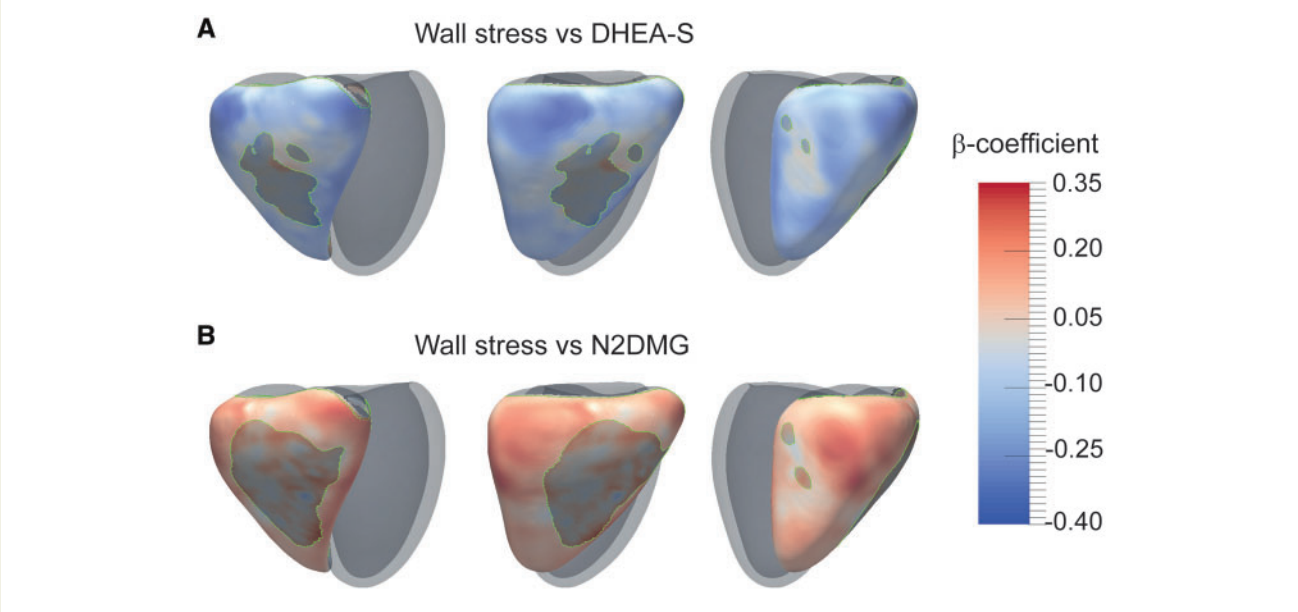

Figure 4 Statistical models of the relationship between right ventricular wall stress and two metabolites in PH patients. The strength of relationship between metabolite concentration and RV end-systolic wall stress is shown by 3D maps of standardized β coefficients with a significance threshold outlined in green ($n = 182$). The RV is shown from three viewpoints with the left ventricle represented in grey. A positive relationship between metabolite level and regional wall stress and is indicated in red and a negative relationship in blue. DHEA-S, dehydroepiandrosterone sulfate; N2DMG, N2,N2-dimethylguanosine.

the dependence of ejection fraction on wall stress rather than as an indicator of RV systolic function.[29]

The strongest associations between metabolite levels and regional wall stress were identified for decreased levels of the sulfated steroid DHEA-S and increased levels of circulating modified nucleosides (N2, N2-dimethylguanosine, N1-methylinosine). Cardiovascular disease patients with lower DHEA-S levels are reported to have a poorer prognosis although the mechanisms for mediating health outcomes

remain unclear,[30] DHEA-S may act as a functional antagonist of glucocorticoids and abnormalities in the regulation and metabolism of insulin, sex hormones, adipokines, and lipids have been found in both animal and human studies of PH.[31] Ours is the first study to report that DHEA-S is also associated with phenotypic evidence of prognostically-important cardiac maladaptation in PH. DHEA prevents and reverses chronic hypoxic PH in rat models and its therapeutic potential in humans is under investigation.[32,33]

Transfer RNA abundance is dynamically regulated and these molecules are involved in adaptive translational pathways and stress signalling in diverse disease states.[34] Our findings indicate that tRNA biology is closely linked to progressive states of RV decompensation across PH disease groups. Significant associations between adverse wall stress patterns and pathways related to cellular energy production were also observed in our population. In PH, the myocardium shifts from oxidative phosphorylation to anaerobic glycolysis.[35] Such metabolic remodelling has been associated with a transition from a compensated to decompensated state in PH,[36] and our findings show that dysfunctional energy metabolism is related to biomechanical overload. Restoration of glucose oxidation by dichloroacetate therapy has recently shown promise as a metabolic approach for reducing mPAP and improving functional capacity.[37] This is one of a growing number of novel strategies to combat the deleterious effects of walls stress in PH that include improving oxygen delivery, restoring mitochondrial function, and modifying neurohormonal modulation.[2]

Limitations

This study has strengths and limitations. Our computational analysis provides a powerful framework for understanding the relationship between RV physiology and putative biomarkers across large PH populations. Our algorithms readily scale to large populations and in future may enable high-throughput screening of disease-modifying molecular pathways across health and disease, as well as a direct use in providing quantitative visualizations of the right ventricle in clinical practice. The models could be further refined with knowledge of fibre orientations and myocardial mechanical properties. The metabolites investigated had been previously shown to discriminate healthy and disease control subjects and independently predict survival—and we found convincing associations between these biomarkers and RV overload in a broader population of PH patients. However, we cannot establish causal interrelationships between these biomarkers and right heart dysfunction, and nor did we have direct tissue or transvenous pulmonary sampling to determine the source or tissue concentrations of these metabolites. Our cohort also represented a relatively diverse cohort receiving a range of standard therapies. Lastly, a significant number of potentially eligible patients did not have CMR near the time of RHC reflecting current clinical practice.

Conclusion

In conclusion, wall stress influences outcomes in PH and is associated with metabolic pathways that report on energy metabolism and cellular stress response. Several of these pathways are tractable as therapeutic targets for reducing wall stress and warrant further investigation.

Supplementary data

Supplementary data are available at *European Heart Journal - Cardiovascular Imaging* online.

Acknowledgements

We are indebted to George Villa and Lavanya Ranganathan for their work on the Translational Research in Pulmonary Hypertension at Imperial College database. The authors would also like to thank all the staff at our MR Facility especially Alaine Berry for her invaluable help with cardiac image analysis.

Funding

This study presents independent research funded by the British Heart Foundation (NH/17/1/32725, RE/13/4/30184, FS/15/59/31839), Academy of Medical Sciences (SGL015/1006), Wellcome Trust (100211/Z/12/Z), and Medical Research Council and supported by the National Institute for Health Research (NIHR) Clinical Research Facility and Biomedical Research Centre at Imperial College London Healthcare NHS Trust and Imperial College London. The views expressed are those of the authors and not necessarily those of the NHS, the NIHR or the Department of Health.

Conflict of interest: none declared.

References

1. Gall H, Felix JF, Schneck FK, Milger K, Sommer N, Voswinckel R *et al*. The Giessen Pulmonary Hypertension Registry: survival in pulmonary hypertension subgroups. *J Heart Lung Transplant* 2017;**36**:957–67.
2. Westerhof BE, Saouti N, van der Laarse WJ, Westerhof N, Vonk Noordegraaf A. Treatment strategies for the right heart in pulmonary hypertension. *Cardiovasc Res* 2017;**113**:1465–73.
3. Vonk Noordegraaf A, Westerhof BE, Westerhof N. The relationship between the right ventricle and its load in pulmonary hypertension. *J Am Coll Cardiol* 2017;**69**:236–43.
4. van de Veerdonk MC, Kind T, Marcus JT, Mauritz GJ, Heymans MW, Bogaard HJ *et al*. Progressive right ventricular dysfunction in patients with pulmonary arterial hypertension responding to therapy. *J Am Coll Cardiol* 2011;**58**:2511–9.
5. Bogaard HJ, Natarajan R, Henderson SC, Long CS, Kraskauskas D, Smithson L *et al*. Chronic pulmonary artery pressure elevation is insufficient to explain right heart failure. *Circulation* 2009;**120**:1951–60.
6. Rhodes CJ, Ghataorhe P, Wharton J, Rue-Albrecht KC, Hadinnapola C, Watson G *et al*. Plasma metabolomics implicates modified transfer RNAs and altered bioenergetics in the outcomes of pulmonary arterial hypertension. *Circulation* 2017;**135**:460–75.
7. Galie N, Humbert M, Vachiery JL, Gibbs S, Lang I, Torbicki A *et al*. 2015 ESC/ERS guidelines for the diagnosis and treatment of pulmonary hypertension. *Rev Esp Cardiol (Engl Ed)* 2016;**69**:177.
8. Simonneau G, Gatzoulis MA, Adatia I, Celermajer D, Denton C, Ghofrani A *et al*. Updated clinical classification of pulmonary hypertension. *J Am Coll Cardiol* 2013;**62**:D34–41.
9. Bai W, Shi W, de Marvao A, Dawes TJ, O'Regan DP, Cook SA *et al*. A bi-ventricular cardiac atlas built from 1000+ high resolution MR images of healthy subjects and an analysis of shape and motion. *Med Image Anal* 2015;**26**:133–45.
10. Kramer CM, Barkhausen J, Flamm SD, Kim RJ, Nagel E. Standardized cardiovascular magnetic resonance (CMR) protocols 2013 update. *J Cardiovasc Magn Reson* 2013;**15**:91.
11. Woodbridge M, Fagiolo G, O'Regan DP. MRIdb: medical image management for biobank research. *J Digit Imaging* 2013;**26**:886–90.
12. Schulz-Menger J, Bluemke DA, Bremerich J, Flamm SD, Fogel MA, Friedrich MG *et al*. Standardized image interpretation and post processing in cardiovascular magnetic resonance: Society for Cardiovascular Magnetic Resonance (SCMR) board of trustees task force on standardized post processing. *J Cardiovasc Magn Reson* 2013;**15**:35.
13. Mam V, Tanbe AF, Vitali SH, Arons E, Christou HA, Khalil RA. Impaired vasoconstriction and nitric oxide-mediated relaxation in pulmonary arteries of hypoxia- and monocrotaline-induced pulmonary hypertensive rats. *J Pharmacol Exp Ther* 2010;**332**:455–62.

14. Aljabar P, Heckemann RA, Hammers A, Hajnal JV, Rueckert D. Multi-atlas based segmentation of brain images: atlas selection and its effect on accuracy. *Neuroimage* 2009;**46**:726–38.
15. Shi W, Lombaert H, Bai W, Ledig C, Zhuang X, Marvao A *et al*. Multi-atlas spectral PatchMatch: application to cardiac image segmentation. *Med Image Comput Comput Assist Interv* 2014;**17(Pt 1)**:348–55.
16. Petitjean C, Zuluaga MA, Bai W, Dacher JN, Grosgeorge D, Caudron J *et al*. Right ventricle segmentation from cardiac MRI: a collation study. *Med Image Anal* 2015;**19**:187–202.
17. Cohen-Steiner D, Morvan J-M. Restricted delaunay triangulations and normal cycle. In: Steve Fortune, ed. *Proceedings of the Nineteenth Annual Symposium on Computational Geometry*. San Diego, CA, USA: ACM; 2003. p312–321.
18. Dawes TJW, de Marvao A, Shi W, Fletcher T, Watson GMJ, Wharton J *et al*. Machine learning of three-dimensional right ventricular motion enables outcome prediction in pulmonary hypertension: a cardiac MR imaging study. *Radiology* 2017;**283**:381–90.
19. Zhong L, Su Y, Yeo SY, Tan RS, Ghista DN, Kassab G. Left ventricular regional wall curvedness and wall stress in patients with ischemic dilated cardiomyopathy. *Am J Physiol Heart Circ Physiol* 2009;**296**:H573–84.
20. Zhang Z, Tendulkar A, Sun K, Saloner DA, Wallace AW, Ge L *et al*. Comparison of Young Laplace law and finite element based calculation of ventricular wall stress: implications for post infarct and surgical ventricular remodeling. *Ann Thorac Surg* 2011;**91**:150–6.
21. Biffi C, de Marvao A, Attard MI, Dawes TJW, Whiffin N, Bai W *et al*. Three-dimensional cardiovascular imaging-genetics: a mass univariate framework. *Bioinformatics* 2018;**34**:97–103.
22. Da Mota B, Fritsch V, Varoquaux G, Banaschewski T, Barker GJ, Bokde AL *et al*. Randomized parcellation based inference. *Neuroimage* 2014;**89**:203–15.
23. Benjamini Y, Hochberg Y. Controlling the false discovery rate—a practical and powerful approach to multiple testing. *J R Stat Soc Series B Methodol* 1995;**57**: 289–300.
24. Benjamini Y, Yekutieli D. Quantitative trait loci analysis using the false discovery rate. *Genetics* 2005;**171**:783–90.
25. Hagger D, Condliffe R, Woodhouse N, Elliot CA, Armstrong IJ, Davies C *et al*. Ventricular mass index correlates with pulmonary artery pressure and predicts survival in suspected systemic sclerosis-associated pulmonary arterial hypertension. *Rheumatology (Oxford)* 2009;**48**:1137–42.
26. Fonseca CG, Backhaus M, Bluemke DA, Britten RD, Chung JD, Cowan BR *et al*. The Cardiac Atlas Project—an imaging database for computational modeling and statistical atlases of the heart. *Bioinformatics* 2011;**27**:2288–95.
27. Sarnoff SJ, Braunwald E, Welch GH Jr, Case RB, Stainsby WN, Macruz R. Hemodynamic determinants of oxygen consumption of the heart with special reference to the tension-time index. *Am J Physiol* 1957;**192**:148–56.
28. Wong YY, Ruiter G, Lubberink M, Raijmakers PG, Knaapen P, Marcus JT *et al*. Right ventricular failure in idiopathic pulmonary arterial hypertension is associated with inefficient myocardial oxygen utilization. *Circ Heart Fail* 2011;**4**:700–6.
29. Quaife RA, Chen MY, Lynch D, Badesch DB, Groves BM, Wolfel E *et al*. Importance of right ventricular end-systolic regional wall stress in idiopathic pulmonary arterial hypertension: a new method for estimation of right ventricular wall stress. *Eur J Med Res* 2006;**11**:214–20.
30. Wu TT, Chen Y, Zhou Y, Adi D, Zheng YY, Liu F *et al*. Prognostic value of dehydroepiandrosterone sulfate for patients with cardiovascular disease: a systematic review and meta-analysis. *J Am Heart Assoc* 2017;**6**:e004896.
31. Pugh ME, Hemnes AR. Metabolic and hormonal derangements in pulmonary hypertension: from mouse to man. *Int J Clin Pract Suppl* 2010;**64**:5–13.
32. Bonnet S, Dumas-de-La-Roque E, Begueret H, Marthan R, Fayon M, Dos Santos P *et al*. Dehydroepiandrosterone (DHEA) prevents and reverses chronic hypoxic pulmonary hypertension. *Proc Natl Acad Sci USA* 2003;**100**:9488–93.
33. Dumas de La Roque E, Savineau JP, Metivier AC, Billes MA, Kraemer JP, Doutreleau S *et al*. Dehydroepiandrosterone (DHEA) improves pulmonary hypertension in chronic obstructive pulmonary disease (COPD): a pilot study. *Ann Endocrinol (Paris)* 2012;**73**:20–5.
34. Kirchner S, Ignatova Z. Emerging roles of tRNA in adaptive translation, signalling dynamics and disease. *Nat Rev Genet* 2015;**16**:98–112.
35. Graham BB, Kumar R, Mickael C, Sanders L, Gebreab L, Huber KM *et al*. Severe pulmonary hypertension is associated with altered right ventricle metabolic substrate uptake. *Am J Physiol Lung Cell Mol Physiol* 2015;**309**:L435–40.
36. Sutendra G, Dromparis P, Paulin R, Zervopoulos S, Haromy A, Nagendran J *et al*. A metabolic remodeling in right ventricular hypertrophy is associated with decreased angiogenesis and a transition from a compensated to a decompensated state in pulmonary hypertension. *J Mol Med* 2013;**91**:1315–27.
37. Michelakis ED, Gurtu V, Webster L, Barnes G, Watson G, Howard L *et al*. Inhibition of pyruvate dehydrogenase kinase improves pulmonary arterial hypertension in genetically susceptible patients. *Sci Transl Med* 2017;**9**:eaao4583.